Design of High Coordination Number Metallomesogens by Decoupling of the Complex-Forming and Mesogenic Groups: Nematic and Lamello-Columnar Mesophases

ARTICLE *in* CHEMISTRY OF MATERIALS · DECEMBER 2005

Impact Factor: 8.35 · DOI: 10.1021/cm0513177

Design of High Coordination Number Metallomesogens by Decoupling of the Complex-Forming and Mesogenic Groups: Nematic and Lamello-Columnar Mesophases

Thomas Cardinaels,[†] Kris Driesen,[†] Tatjana N. Parac-Vogt,[†] Benoît Heinrich,[‡] Cyril Bourgogne,[‡] Daniel Guillon,[‡] Bertrand Donnio,*[,‡] and Koen Binnemans*[,†]

Department of Chemistry, Katholieke Universiteit Leuven, Celestijnenlaan 200F, B-3001 Leuven, Belgium, and Institut de Physique et Chimie des Matériaux de Strasbourg—Groupe des Matériaux Organiques, UMR 7504 CNRS-Université Louis Pasteur, BP43, 23 rue du Loess, F-67034 Strasbourg Cedex 2, France

Received June 19, 2005. Revised Manuscript Received August 26, 2005

Liquid-crystalline complexes of rhenium(I), yttrium(III), lanthanum(III), neodymium(III), samarium(III), europium(III), erbium(III), and ytterbium(III) were obtained by coupling mesogenic 4-cyanobiphenyl groups via a long alkyl spacer to a substituted imidazo[4,5-f]-1,10-phenanthroline, which acts as the coordinating group. In the case of the rare-earth complexes, 2-thenoyltrifluoroacetonate was used as the coligand. The rhenium(I) complexes contain the bromotricarbonylrhenium(I) moiety. All the rare-earth complexes exhibit a nematic phase, whereas the rhenium(I) complexes and the imidazole-bearing phenanthroline derivatives show a nematic or a lamellar columnar phase, depending on the number of attached mesogenic groups. The phase structures of the lamellar columnar phases are discussed and described on the basis of both X-ray diffraction data and dynamic molecular modeling. The lanthanide complexes are highly luminescent in the solid phase and as a solution in a nematic liquid-crystal host (5CB). The approach discussed in this paper can be generalized to obtain other high coordination number metallomesogens.

Introduction

Metal-containing liquid crystals (*metallomesogens*) are multifunctional molecular materials.[1] These interesting compounds have properties that are typical for both liquid crystals and d-group transition metals or rare earths. In the mesophase, the molecules of metallomesogens are ordered like in classic organic liquid crystals, and their optical, magnetic, electric, and mechanical properties are anisotropic. But at the same time, metallomesogens can have the redox activity or can exhibit the magnetic and optical properties of d-block or f-block metals. The first metallomesogens were designed in such a way that they mimicked the shape of rodlike (calamitic) organic liquid crystals. To exhibit a mesophase, the shape anisotropy of the complex must be sufficient. The choice of the metal ion was restricted previously to those ions that are able to form complexes with a linear or a square planar coordination. Therefore, many of the earlier described metallomesogens contain rhodium(I), iridium(I), nickel(II), copper(II), palladium(II), platinum(II), or silver(I) as the central metal ion. It is a challenge to design metallomesogens with coordination geometries other than linear or square planar ones. Only few metallomesogens have a tetrahedral metal center, because a tetrahedral coordination geometry is difficult to combine with the requirement of structural anisotropy and good lateral interactions for mesophase formation.[2] Due to the stronger geometrical constraints, it is even more difficult to obtain metallomesogens with a coordination number of six or even higher.[3] The first metallomesogens with an octahedral coordination sphere were the 1,4,7-triazacyclononane tricarbonyl and trichloro metal complexes ($ML(CO)_3$, with M = W, Cr, and Mo, and $FeLCl_3$) described by Lattermann and co-workers.[4] Bruce and co-workers prepared the first octahedral metallomesogens with a calamitic shape.[5] Ghedini and co-workers described octahedral platinum(IV) complexes.[6] Binnemans, Bruce,

* Corresponding authors. E-mail: Koen.Binnemans@chem.kuleuven.be (K.B.); bdonnio@ipcms.u-strasbg.fr (B.D.).

[†] Katholieke Universiteit Leuven.

[‡] Université Louis Pasteur.

(1) (a) Giroud-Godquin, A. M.; Maitlis, P. M. *Angew. Chem., Int. Ed. Engl.* **1991**, *30*, 375. (b) Espinet, P.; Esteruelas, M. A.; Oro, L. A.; Serrano, J. L.; Sola, E. *Coord. Chem. Rev.* **1992**, *117*, 215. (c) Hudson, S. A.; Maitlis, P. M. *Chem. Rev.* **1993**, *93*, 861. (d) *Metallomesogens, Synthesis, Properties and Applications*; Serrano, J. L., Ed.; VCH: Weinheim, Germany, 1996. (e) Bruce, D. W. In *Inorganic Materials*, 2nd ed.; Bruce, D. W., O'Hare, D., Eds.; Wiley: Chichester, U.K., 1996; Chapter 8, p 429. (f) Donnio, B.; Bruce, D. W. *Struct. Bonding (Berlin)* **1999**, 193−247. (g) Binnemans, K.; Görller-Walrand, C. *Chem. Rev.* **2002**, *102*, 2303. (h) Donnio, B.; Guillon, D.; Deschenaux, R.; Bruce, D. W. In *Comprehensive Coordination Chemistry II*; McCleverty, J. A., Meyer, T. J., Fujita, M., Powell, A., Creutz, C., Eds.; Elsevier: Oxford, 2003; Vol. 7, Chapter 7.9, pp 357−627.

(2) (a) Neve, F.; Ghedini, M.; De Munno, G.; Levelut, A. M. *Chem. Mater.* **1995**, *7*, 688. (b) Douce, L.; El-ghayoury, A.; Skoulios, A.; Ziessel, R. *Chem. Commun.* **1999**, 2033. (c) Ziessel, R.; Douce, L.; El-ghayoury, A.; Harriman, A.; Skoulios, A. *Angew. Chem., Int. Ed.* **2000**, *39*, 1489. (d) Giménez, R.; Manrique, A. B.; Uriel, S.; Barbera, J.; Serrano, J. L. *Chem. Commun.* **2004**, 2064.

(3) Bruce, D. W. *Adv. Mater.* **1994**, *6*, 699.

(4) (a) Lattermann, G.; Schmidt, S.; Kleppinger, R.; Wendorf, J. H. *Adv. Mater.* **1992**, *4*, 30. (b) Schmidt, S.; Lattermann, G.; Kleppinger, R.; Wendorff, J. H. *Liq. Cryst.* **1994**, *16*, 693. (c) Walf, G. H.; Benda, R.; Litterst, F. J.; Stebani, U.; Schmidt, S.; Lattermann, G. *Chem. Eur. J.* **1998**, *4*, 93.

(5) (a) Bruce, D. W.; Liu, X. H. *J. Chem. Soc., Chem. Commun.* **1994**, 729. (b) Morrone, S.; Harrison, G.; Bruce, D. W. *Adv. Mater.* **1995**, *7*, 665. (c) Morrone, S.; Guillon, D.; Bruce, D. W. *Inorg. Chem.* **1996**, *35*, 7041.

10.1021/cm0513177 CCC: $30.25
Published on Web 11/25/2005

Galyametdinov and co-workers described rare-earth-containing liquid crystals, which have a coordination number of eight or nine.[7] Other types of rare-earth-containing liquid crystals have then been studied by the research groups of Piguet and Bünzli,[8] and Serrano.[9] Swager made mesomorphic β-diketonate complexes with an octahedral,[10] and with a square antiprismatic coordination.[11] Also ferrocene-containing liquid crystals are examples of high coordination number metallomesogens.[12] A popular approach to overcome the disturbance of the rodlike shape of the ligands after complex formation with a bulky transition-metal fragment is to increase the number of phenyl groups in order to increase the anisotropy of the ligands.[13] Inevitably, this will lead to higher transition temperatures and to a lower thermal stability of the metal complexes. One can also increase the number of alkyl chains attached to the coordination unit, but in this case the metal complexes exhibit columnar mesophases as a rule.[10,11] It is evident that alternative approaches to obtain high coordination number metallomesogens with nematic or smectic mesophases are a scientific challenge, especially when these compounds ought to have low or moderate transition temperatures. As far as this matter is concerned, particularly the work of Deschenaux is inspiring, because he found methods to obtain liquid-crystalline C_{60} fullerenes,[14] the bulky fullerene being incompatible with the requirements for structural anisotropy. Typically, classical mesogenic groups such as cholesteryl or cyanobiphenyl groups are linked to the fullerene moiety by long flexible chains. Saez and co-workers were able to prepare liquid-crystalline clusters on the basis of octasilsesquioxane by using a similar strategy.[15]

In this paper, we describe the design of high coordination number metallomesogens, which exhibit nematic or lamellar columnar phases. The basic idea is to decouple the mesogenic groups from the metal-coordinating group by a flexible spacer. In this way, the system resembles to a covalent host−guest system where the metal complex (the guest) is dissolved in the liquid-crystal host, but phase separation is prevented by covalently linking the metal complex to the mesogenic moiety. This approach is illustrated for rhenium(I) and rare-earth complexes of 2-arylimidazo[4,5-f]-1,10-phenanthroline derivatives. The ligand is bearing one, two, or three cyanobiphenyl groups separated from the coordinating core by long alkyl chains. The rhenium(I) compounds are six-coordinate metallomesogens, and the rare-earth complexes are eight-coordinate systems. We investigated the influence of the number of mesogenic groups and of the nature of the metal ion on the mesomorphic properties of the complexes. The rare-earth complexes are not only luminescent themselves, but they are also completely soluble in the liquid crystal 4′-pentyl-4-cyanobiphenyl (5CB). This allows obtaining strongly luminescent liquid-crystal mixtures.

Results and Dissusion

Synthesis of Ligands and Complexes. The inspiration to develop the materials presented in this paper came from previous work on liquid-crystalline rare-earth complexes with β-diketonate ligands. Mesomorphism was observed in adducts of long-chain salicylaldimine Schiff bases with tris(dibenzoylmethanato)lanthanide(III) complexes.[7e,16] Similarly, highly ordered smectic mesophases were found in complexes of rare earths with mesogenic β-diketonates.[17] Mesomorphic analogues of the tris(2-thenoyltrifluoroacetonato)(1,10-phenanthroline)lanthanide(III) complexes, [Ln(tta)$_3$(phen)] were synthesized, because of the good luminescence performance of these complexes. For instance, the europium(III) complex [Eu(tta)$_3$(phen)] is one of the best known red-emitting molecular luminescent materials (Htta = 2-thenoyltrifluoroacetone or 4,4,4-trifluoro-1-(thiophen-2-yl)butane-1,3-dione).[18] The complexes [Nd(tta)$_3$(phen)],

(6) (a) Ghedini, M.; Pucci, D.; Crispini, A.; Barberio, G. *Organometallics* **1999**, *18*, 2116. (b) Ghedini, M.; Pucci, D.; Barberio, G. *Liq. Cryst.* **2000**, *27*, 1277.

(7) (a) Galyametdinov, Yu. G.; Ivanova, G. I.; Ovchinnikov, I. V. *Bull. Acad. Sci. USSR, Div. Chem. Sci. (Engl. Transl.)* **1991**, *40*, 1109; *Izv. Akad. Nauk SSSR, Ser. Khim.* **1991**, 1232. (b) Galyametdinov, Yu.; Athanassopoulou, M. A.; Griesar, K.; Kharitonova, O.; Soto Bustamante, E. A.; Tinchurina, L.; Ovchinnikov, I.; Haase, W. *Chem. Mater.* **1996**, *8*, 922. (c) Binnemans, K.; Bruce, D. W.; Collinson, S. R.; Van Deun, R.; Galyametdinov, Yu. G.; Martin, F. *Philos. Trans. R. Soc. London, Ser. A* **1999**, *357*, 3063. (d) Binnemans, K.; Galyametdinov, Yu. G.; Van Deun, R.; Bruce, D. W.; Collinson, S. R.; Polishchuk, A. P.; Bikchantaev, I.; Haase, W.; Prosvirin, A. V.; Tinchurina, L.; Litvinov, I.; Gubajdullin, A.; Rakhmatullin, A.; Uytterhoeven, K.; Van Meervelt, L. *J. Am. Chem. Soc.* **2000**, *122*, 4335. (e) Binnemans, K.; Lodewyckx, K. *Angew. Chem.* **2001**, *113*, 248; *Angew. Chem., Int. Ed.* **2001**, *40*, 242. (f) Binnemans, K.; Lodewyckx, K.; Donnio, B.; Guillon, D. *Chem. Eur. J.* **2002**, *8*, 1101. (g) Binnemans, K.; De Feyter, S.; De Schryver, F. C.; Donnio, B.; Guillon, D. *Chem. Mater.* **2003**, *15*, 2930.

(8) (a) Nozary, H.; Piguet, C.; Rivera, J.-P.; Tissot, P.; Morgantini, P.-Y.; Weber, J.; Bernardinelli, G.; Bünzli, J.-C. G.; Deschenaux, R.; Donnio, B.; Guillon, D. *Chem. Mater.* **2002**, *14*, 1075. (b) Terazzi, E.; Benech, J. M.; Rivera, J. P.; Bernardinelli, G.; Donnio, B.; Guillon, D.; Piguet, C. *Dalton Trans.* **2003**, 769. (c) Suarez, S.; Mamula, O.; Imbert, D.; Piguet, C.; Bünzli, J. C. G. *Chem. Commun.* **2003**, 1226. (d) Guillet, E.; Imbert, D.; Scopelliti, R.; Bünzli, J. C. G. *Chem. Mater.* **2004**, *16*, 4063. (e) Terazzi, E.; Torelli, S.; Bernardinelli, G.; Rivera, J.-P.; Benech, J.-M.; Bourgogne, C.; Donnio, B.; Guillon, D.; Imbert, D.; Bünzli, J.-C. G.; Pinto, A.; Jeannerat, D.; Piguet, C. *J. Am. Chem. Soc.* **2005**, *127*, 888.

(9) Marcos, M.; Omenat, A.; Barbera, J.; Duran, F.; Serrano, J. L. *J. Mater. Chem.* **2004**, *14*, 3321.

(10) (a) Zheng, H.; Swager, T. M. *J. Am. Chem. Soc.* **1994**, *116*, 761. (b) Swager, T. M.; Zheng, H. *Mol. Cryst. Liq. Cryst.* **1995**, *260*, 301. (c) Trzaska, S. T.; Hsu, H. F.; Swager, T. M. *J. Am. Chem. Soc.* **1999**, *121*, 4518; Corrigendum, 4544.

(11) Trzaska, S. T.; Zheng, H.; Swager, T. M. *Chem. Mater.* **1999**, *11*, 130.

(12) Deschenaux, R.; Goodby, J. W. Ferrocene-Containing Thermotropic Liquid Crystals. In *Ferrocene: Homogeneous Catalysis, Organic Synthesis, Materials Science*; Togni, A., Hayashi, T., Eds.; VCH: Weinheim, Germany, 1995; Chapter 9, pp 471−495.

(13) (a) Rowe, K. E.; Bruce, D. W. *J. Mater. Chem.* **1998**, *8*, 331. (b) Rowe, K. E.; Bruce D. W. *J. Chem. Soc., Dalton Trans.* **1996**, 3913. (c) Rowe, K. E.; Bruce, D. W. *Mol. Cryst. Liq. Cryst.* **1999**, *326*, 15. (d) Jacq, P.; Malthête, J. *Liq. Cryst.* **1996**, *21*, 291. (e) Campillos, E.; Deschenaux, R.; Levelut, A. M.; Ziessel, R. *J. Chem. Soc., Dalton Trans.* **1996**, 2533. (f) Seo, J. S.; Yoo, Y. S.; Choi, M. G. *J. Mater. Chem.* **2001**, *11*, 1332.

(14) (a) Chuard, T.; Deschenaux, R. *Helv. Chim. Acta* **1996**, *79*, 736. (b) Chuard, T.; Deschenaux, R.; Hirsch, A.; Schönberger, H. *Chem. Commun.* **1999**, 2103. (c) Dardel, B.; Deschenaux, R.; Even, M.; Serrano, E. *Macromolecules* **1999**, *32*, 5193. (d) Dardel, B.; Guillon, D.; Heinrich, B.; Deschenaux, R. *J. Mater. Chem.* **2001**, *11*, 2814.

(15) (a) Mehl, G. H.; Saez, I. M. *Appl. Organomet. Chem.* **1999**, *13*, 261. (b) Saez, I. M.; Goodby, J. W. *J. Mater. Chem.* **2001**, *11*, 2845. (c) Saez, I. M.; Goodby, J. W. *Liq. Cryst.* **1999**, *26*, 1101. (d) Saez, I. M.; Goodby, J. W. *J. Mater. Chem.* **2005**, *15*, 26.

(16) Binnemans, K.; Lodewyckx, K.; Parac-Vogt, T. N.; Van Deun, R.; Goderis, B.; Tinant, B.; Van Hecke, K.; Van Meervelt, L. *Eur. J. Inorg. Chem.* **2003**, *16*, 3028.

(17) Galyametdinov, Yu. G.; Malykhina, L. V.; Haase, W.; Driesen, K.; Binnemans, K. *Liq. Cryst.* **2002**, *29*, 1581.

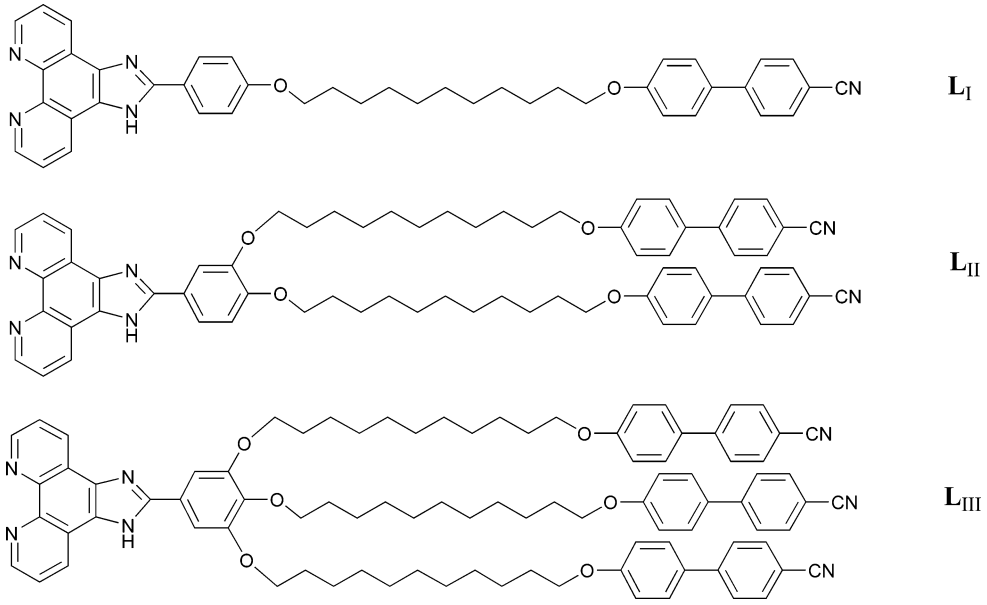

Figure 1. Overview of the imidazo[4,5-f]1,10-phenanthroline ligands.

[Er(tta)$_3$(phen)], and [Yb(tta)$_3$(phen)] emit in the near-infrared region of the electromagnetic spectrum. Taking into account the structure of the 2-thenoyltrifluoroacetonate ligand, it is difficult to induce mesomorphism in the [Ln(tta)$_3$(phen)] complexes by modification of the β-diketonate ligand. Therefore, modification has to be made by functionalization of the 1,10-phenanthroline moiety. The most reactive positions in 1,10-phenanthroline are the 5 and 6 positions. The first trials we made was by using 5-amino-1,10-phenanthroline. This molecule was previously used to attach [Eu(tta)$_3$(phen)] to a sol−gel silica matrix,[19] or to a Merrifield resin.[20] However, the low solubility in common organic solvents and the low photochemical stability of 5-amino-1,10-phenanthroline render its chemistry rather difficult and impractical. In contrast, 1,10-phenanthroline-5,6-dione is a more convenient starting product. 1,10-Phenanthroline is oxidized to 1,10-phenanthroline-5,6-dione according to a method described by Hiort et al.,[21] followed by the transformation of the dione to the 2-arylimidazo[4,5-f]1,10-phenanthrolines by reaction with a substituted benzaldehyde and ammonium acetate in hot glacial acetic acid. The synthetic route is similar to the method of Steck and Day for the preparation of 2-substituted phenanthrimidazoles.[22] By choosing different substituents on the benzaldehyde, the structure and thus the mesophase behavior of the corresponding ligands and metal complexes can in principle be tuned. Although a single compound can be transformed into a mesogenic analogue by attaching for example long alkyl chains, we have selected another methodology, namely by attaching mesogenic groups via a long alkyl chain to the 1,10-phenanthroline derivative. The mesogenic group in this case is a cyanobiphenyl group, linked to the alkyl chain by an ether linkage group. In this respect, 4′-hydroxy-4-biphenylcarbonitrile is a very useful mesogenic building block to design large liquid-crystalline compounds. We have chosen a flexible alkyl chain with eleven carbon atoms. Although different approaches are possible, we coupled 4′-hydroxy-4-biphenylcarbonitrile and 11-bromo-undecanol via the OH group by a Mitsunobu reaction,[23] so that the unit consisting of the flexible chain and the mesogenic group can be coupled to a hydroxybenzaldehyde by a classic Williamson ether reaction. For the Mitsunobu reaction, diisopropyl azodicarboxylate (DIAD) was preferred to diethyl azodicarboxylate (DEAD) as the reagent, because DIAD is more convenient and safer to use. The mesomorphic properties of 4′-(10-bromoundecyloxy)-4-cyanobiphenyl (**2**) have been described by other authors in the past.[24] Three different hydroxybenzaldehydes were used in this study: 4-hydroxybenzaldehyde, 3,4-dihydroxybenzaldehyde, and 3,4,5-trihydroxybenzaldehyde. Depending on the hydroxybenzaldehyde used, one, two, or three mesogenic groups could be coupled via a flexible chain to the substituted 1,10-phenanthroline. An overview of the ligands is given in Figure 1. Their synthesis is described in the Supporting Information. A crystal structure of the methanol adduct of 2-phenylimidazo[4,5-f]-1,10-phenanthroline showed that all the 19 carbon atoms and the 4 nitrogen atoms are coplanar,[25] so it is very likely that the core of our phenan-

(18) (a) Zhong, G. L.; Kim, K.; Jin, J. I. *Synth. Met.* **2002**, *129*, 193. (b) Adachi, C.; Baldo, M. A.; Forrest, S. R. *J. Appl. Phys.* **2000**, *87*, 8049. (c) Sano, T.; Fujita, M.; Fujii, T.; Hamada, Y.; Shibata, K.; Kuroki, K. *Jpn. J. Appl. Phys.* **1995**, *34*, 1883. (d) Li, H. H.; Inoue, S.; Machida, K.; Adachi, G. *Chem. Mater.* **1999**, *11*, 3171. (e) Kido, J.; Okamoto, Y. *Chem. Rev.* **2002**, *102*, 2357. (f) Binnemans, K. Rare-Earth β-Diketonates. In *Handbook on the Physics and Chemistry of Rare Earths*; Gschneidner, K. A., Bünzli, J. C. G., Jr., Pecharsky, V. K., Eds.; Elsevier: Amsterdam, 2005; Vol. 35, Chapter 225, pp 107−272.

(19) (a) Binnemans, K.; Lenaerts, P.; Driesen, K.; Görller-Walrand, C. *J. Mater. Chem.* **2004**, *14*, 191. (b) Lenaerts, P.; Ryckebosch, E.; Driesen, K.; Van Deun, R.; Nockemann, P.; Görller-Walrand, C.; Binnemans, K. *J. Lumin.* **2005**, *114*, 77.

(20) Lenaerts, P.; Driesen, K.; Van Deun, R.; Binnemans, K. *Chem. Mater.* **2005**, *17*, 2148.

(21) Hiort, C.; Lincoln, P.; Norden, B. *J. Am. Chem. Soc.* **1993**, *115*, 3448.

(22) Steck, E. A.; Day, A. R. *J. Am. Chem. Soc.* **1943**, *65*, 452.

(23) Mitsunobu, O. *Synthesis* **1981**, 1.

(24) (a) Imrie, C. T.; Karasz, F. E.; Attard, G. S. *J. Macromol. Sci., Part A* **1994**, *31*, 1221. (b) Everaars, M. D.; Marcelis, A. T. M.; Sudholter, E. J. R. *Langmuir* **1996**, *12*, 3964. (c) Percec, V.; Asandei, A. D.; Hill, D. H.; Crawford, D. *Macromolecules* **1999**, *32*, 2597. (d) Cook, A.; Badriya, S.; Greenfield, S.; McKeown, N. B. *J. Mater. Chem.* **2002**, *12*, 2675. (e) Kouwer, P. H. J.; Mehl, G. H. *J. Am. Chem. Soc.* **2003**, *125*, 11172.

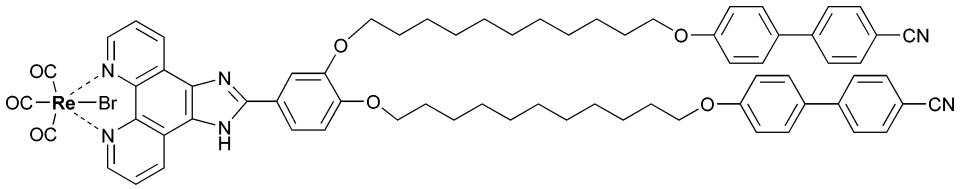

Figure 2. Rhenium(I) complex of ligand $\mathbf{L}_{II}$.

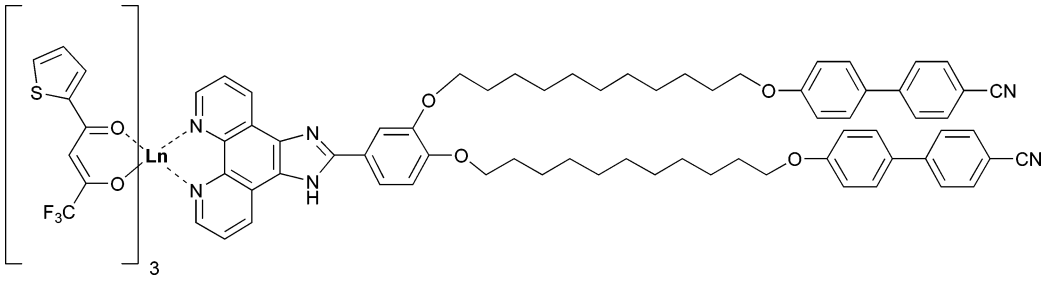

Figure 3. Rare-earth complexes of ligand $\mathbf{L}_{II}$ (Ln = Y, La, Nd, Sm, Eu, Er, Yb).

throline derivatives is flat as well. From the analysis of the bound lengths, it was concluded that the molecule is very extensively conjugated. The 2-arylimidazo[4,5-f]-1,10-phenanthrolines have a tendency to form strong H-bonded adducts with methanol or other lower alcohols. For this reason, it is preferable to exclude these solvents from the synthetic procedure if one wants to obtain solvent-free 2-arylimidazo[4,5-f]-1,10-phenanthrolines.

Complexes of rhenium(I) and of trivalent rare-earth ions were prepared from the different 2-arylimidazo[4,5-f]-1,10-phenanthroline ligands. Rhenium(I) was chosen rather than group 10 metals since they tend to give more thermally and chemically stable complexes with ligands derived from 2,2′-bipyridine and 1,10-phenanthroline and since mesophases could be observed for these complexes as found by Bruce and co-workers.[13b,13c,26] Another interesting feature is that the rhenium(I) complexes containing the bulky $Re(CO)_3Br$ fragment have a large dipole moment due to the polar Re−Br bond. This dipole, in combination with the number of 4-cyanobiphenyl groups attached, is expected to influence the arrangement of the molecules in the mesophase and the solid phase. The trivalent rare-earth ions were selected in such a way that the steady decrease of the ionic radius over the lanthanide series (*lanthanide contraction*) was reflected; indeed, the decrease of the ionic radius often influences the thermal properties of the compounds.[1g] Moreover, the choice of rare-earth ions was also determined by the physical properties of the ions: lanthanum(III) and yttrium(III) compounds are diamagnetic, so that they can be conveniently studied by NMR techniques. The neodymium(III), samarium(III), europium(III), erbium(III), and ytterbium(III) ions were chosen because of their photoluminescent properties.

Rhenium(I), yttrium(III), lanthanum(III), neodymium(III), samarium(III), europium(III), erbium(III), and ytterbium(III) complexes of ligands $\mathbf{L}_I$, $\mathbf{L}_{II}$, and $\mathbf{L}_{III}$ were therefore prepared (see the Supporting Information). The rhenium(I) complexes were obtained by reaction between the ligand and rhenium pentacarbonyl bromide in toluene (molar ratio 1:1). The rare-earth complexes were prepared by reaction of the ligand and a tris(2-thenoyltrifluoroacetonate)lanthanide dihydrate complex, $[Ln(tta)_3(H_2O)_2]$ (Ln = Y, La, Nd, Sm, Eu, Er, Yb), in chloroform (molar ratio 1:1). The complexes were characterized by CHN elemental analysis, by IR spectroscopy, and by electrospray mass spectrometry (ESI-MS). The structures of complexes $[Re(CO)_3Br\mathbf{L}_{II}]$ and $[Ln(tta)_3\mathbf{L}_{II}]$ ((Ln = Y, La, Nd, Sm, Eu, Er, Yb) are shown in Figures 2 and 3, respectively. It should be mentioned that all ligands and metal complexes were obtained as monohydrates. The bonded water molecule could not be removed, even not after a long drying period in a vacuum oven (below the melting point of the compounds).

Solution Studies. The coordination mode of the metal ion in solution was examined by measuring one- and two-dimensional proton NMR spectra of the diamagnetic $[Re(CO)_3Br\mathbf{L}_{II}]$ and $[Ln(tta)_3\mathbf{L}_{II}]$ (Ln = Y, La) complexes which were then compared to the proton NMR spectra of the ligands $\mathbf{L}_{II}$ and that of 2-thenoyltrifluoroacetone (Htta). The proton NMR resonances of the free ligand $\mathbf{L}_{II}$ are sharp and show the expected splitting pattern (see the Supporting Information). Upon coordination to the rhenium(I)-containing moiety $Re(CO)_3Br$, the proton signals of the 1,10-phenantroline unit shifted between 0.14 and 0.39 ppm downfield, as compared to the corresponding protons of the free ligand. The magnitude of the observed downfield shifts is consistent with the 1,10-phenantroline ligand coordination to rhenium(I).[27,28] While the proton signals of the aryl group attached to the imidazole ring also experienced a slight downfield shift, the aromatic protons of cyanobiphenyl groups were unaffected by the coordination to rhenium(I), indicating that there was no interaction between the cyano group and the metal center. In the proton NMR spectrum of the $[La(tta)_3\mathbf{L}_{II}]$ complex the resonances of 1,10-phenantroline were broadened and shifted between 0.11 and 0.35 ppm downfield compared to those of the free ligand. These downfield shifts are compa-

(25) (a) Lin, H. W.; Zhu, W. X. *Chin. J. Chem.* **2003**, *21*, 1054. (b) Wu, J. Z.; Wang, L.; Yang, G.; Ji, L. N.; Katsaros, N.; Koutsodimou, A. *Cryst. Res. Technol.* **1996**, *31*, 857.
(26) (a) Bruce, D. W.; Liu, H. X., *Liq. Cryst.* **1995**, *18*, 156. (b) Date, R. W.; Fernandez Iglesias, E.; Rowe, K. E.; Elliott, J. M.; Bruce, D. W. *Dalton Trans.* **2003**, 1914.
(27) Wrighton, M. S.; Morse, D. L. *J. Am. Chem. Soc.* **1974**, *96*, 998.
(28) Itokazu, M. K.; Polo, A. S.; De Faria, D. L. A.; Bignozzi, C. A.; Iha, N. Y. I. *Inorg. Chim. Acta* **2001**, *313*, 149.

rable to the values found for other diamagnetic lanthanum(III) complexes of 1,10-phenantroline.[29,30] No signals of free 1,10-phenantroline were observed in the spectrum. Similarly, no evidence for free 2-thenoyltrifluoroacetone was observed. Uncoordinated 2-thenoyltrifluoroacetone exists in $CDCl_3$ solutions 100% in the enol form, displaying a prominent enol proton resonance at 14.84 ppm. Upon complexation of the ligand to lanthanum(III) in [La(tta)$_3$**L**$_{II}$], this resonance disappears which indicates full coordination of the 2-thenoyltrifluoroacetonate ligand to the lanthanum(III) ion. At room temperature, the proton NMR resonances of the 1,10-phenantroline unit in the [Y(tta)$_3$**L**$_{II}$] complex was significantly broadened, while the methine signal at 6.33 pm was rather sharp. Variable temperature proton NMR spectra of [Y(tta)$_3$**L**$_{II}$] were measured in order to investigate the possible dynamic process which led to the broadening of the NMR resonances. Upon lowering the temperature to −25 °C, the 1,10-phenantroline peaks sharpened while the methine peak of the 2-thenoyltrifluoroacetonate ligand broadened into a hump consisting of at least three overlapping signals (see the Supporting Information). The dynamic processes which take place in solution of the [Y(tta)$_3$**L**$_{II}$] complex are difficult to elucidate. These may involve exchange of the ligands or partial dissociation of the 1,10-phenantroline derivative and of one or more 2-thenoyltrifluoroacetonate ligands from the yttrium(III) ion. In addition, conformational freezing of the three β-diketonate ligands or other coordination modes could be also possible. Variable temperature NMR spectra of the [La(tta)$_3$**L**$_{II}$] complex also showed splitting of the 2-thenoyltrifluoroacetonate methine resonances upon lowering the temperature to −25 °C, indicating partial dissociation of the 2-thenoyltrifluoroacetonate ligands from lanthanum(III). Similar dynamic behavior was previously observed in solutions of other rare-earth complexes with β-diketonate ligands.[16]

Thermal Behavior. The thermal behavior of the different benzaldehyde precursors, phenanthroline derivatives, and metal complexes was investigated by differential scanning calorimetry (DSC), polarizing optical microscopy (POM), and by small-angle X-ray diffraction on powder samples. Determination of accurate transition temperatures was not easy because no well-resolved thermograms of the imidazo-[4,5-f]-1,10-phenanthroline ligands and of the corresponding metal complexes were obtained by DSC. The absence of a distinct melting peak can be attributed to the low crystallinity of the compounds, a consequence of their nonlinear, oligomeric-like structures, some of them being even obtained as waxy solids after synthesis. The three precursor aldehydes (3, 4, 5) exhibit a nematic phase, which is monotropic for 3, and enantiotropic for 4 and 5, though over a narrow temperature range (see the Supporting Information). Quite interestingly, both the ligands **L**$_I$ and **L**$_{II}$ and all their metal−adduct derivatives, except the [Re(CO)$_3$Br**L**$_I$] complex, exhibit a N phase with similar transition temperatures with the melting points ranging between 75 and 92°C and the clearing temperatures between 124 and 138 °C, and with an average mesomorphic temperature range of about 40 to 50 °C. A slight decrease of the transition temperatures, but with a constant mesomorphic temperature domain, was achieved with the ligand **L**$_{III}$ and the rhenium(I) derivative [Re(CO)$_3$Br**L**$_{III}$]. However, the europium(III) complex of this ligand showed a mesophase over a small temperature range of only 9 °C. In most cases, it was only possible to observe a defect texture after inducing birefringence by pressing with a needle on the glass coverslips of the microscope preparations. Some of the samples tend to orient nearly perpendicular to the glass slide surface to give a homeotropic texture, and by pressing the glass coverslips this orientation is disrupted. An overview of the transition temperatures is given in Table 1.

Table 1. Transition Temperatures and Mesophases of the Substituted Imidazo[4,5-f]-1,10-phenanthroline Ligands and the Corresponding Metal Complexes

compound	transition temps (°C)[a]	temp range, ΔT (°C)
L$_I$	Cr·80·N·124·I	44
[Re(CO)$_3$Br**L**$_I$]	Cr·260 (·N·158)·I	
[Nd(tta)$_3$**L**$_I$]	Cr·86·N·138·I	52
[Eu(tta)$_3$**L**$_I$]	Cr·89·N·138·I	49
L$_{II}$	Cr·75·N·128·I	53
[Re(CO)$_3$Br**L**$_{II}$]	Cr·81 (·SmA$_{Col}$·65)·N·128·I	47
[Y(tta)$_3$**L**$_{II}$]	Cr·89·N·127·I	38
[La(tta)$_3$**L**$_{II}$]	Cr·84·N·124·I	40
[Nd(tta)$_3$**L**$_{II}$]	Cr·85·N·124·I	39
[Sm(tta)$_3$**L**$_{II}$]	Cr·86·N·124·I	38
[Eu(tta)$_3$**L**$_{II}$]	Cr·86·N·125·I	39
[Er(tta)$_3$**L**$_{II}$]	Cr·90·N·127·I	37
[Yb(tta)$_3$**L**$_{II}$]	Cr·92·N·127·I	35
L$_{III}$	Cr·48·SmA$_{Col}$·94·I	46
[Re(CO)$_3$Br**L**$_{III}$]	Cr·49·Col$_r$L·105·I	56
[Eu(tta)$_3$**L**$_{III}$]	Cr·83·N·92·I	9

[a] Abbreviations: Cr = crystalline or semicrystalline phase; N = nematic phase; SmA$_{Col}$ = unconventional smectic A phase with an in-plane short-range ordered columnar stacking; Col$_r$L = unconventional smectic phase with a long-range ordered 2D columnar packing (see text); I = isotropic liquid.

All the compounds exhibit enantiotropic mesophases, except the rhenium(I) complex [Re(CO)$_3$Br**L**$_I$], which forms a monotropic nematic mesophase. Deduced from observations by polarizing optical microscopy, the rare-earth complexes systematically exhibit a nematic phase. The characteristic texture was recognized by the formation of Schlieren textures with two- and four-brushes point defects, along with large homeotropic areas. No sign of an additional more ordered phase was detected. X-ray diffraction experiments on powder samples were sufficient to confirm the correct assignment of the nematic phase. Indeed, the observation of a broad scattering signal in the small-angle region instead of the presence of sharp intense peaks in the temperature range of the mesophase confirmed the absence of 1D or 2D long-range correlated positional ordering. This broad signal corresponds to lateral short-range molecular correlations of the order of the molecular length, typical of the orientational nematic ordering. In the wide-angle part, the signal at ca. 4.5 Å, attributed to the lateral short-range order of the molten chains and cyanobiphenyl moieties, was also observed.

As for the three imidazo[4,5-f]-1,10-phenanthroline ligands, both **L**$_I$ and **L**$_{II}$ exhibit a nematic phase, whereas in the case of **L**$_{III}$, the crystal phase transforms on heating into a smectic-like phase with a short-range ordering of columns (vide infra). The nematic phase of **L**$_I$ and **L**$_{II}$ was identified on

(29) Khan, A. A.; Saxena, A. K.; Iftikhar, K. *Polyhedron* **1997**, *16*, 4143.
(30) Iftikhar, K. *Polyhedron* **1996**, *15*, 1113.

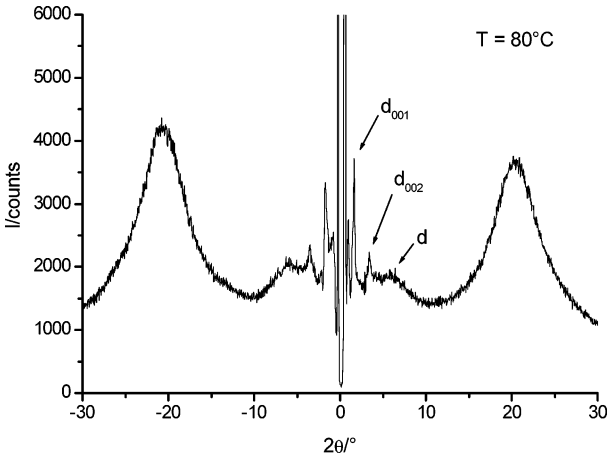

Figure 4. X-ray pattern of the SmA_{Col}-type phase of $\mathbf{L}_{III}$ at 80 °C. The following diffraction peaks are observed: $d_{001} = 50.0$ Å, $d_{002} = 25.0$ Å, $d = 14.0$ Å, and a broad scattering at 4.5 Å.

the basis of its optical texture observed by polarizing optical microscopy, showing Schlieren textures with two and four brushes, whereas for $\mathbf{L}_{III}$, no characteristic texture was obtained, except from the presence of large homeotropic areas. In the case of the nematogenic ligands $\mathbf{L}_I$ and $\mathbf{L}_{II}$, X-ray diffraction patterns resembled those described above for the rare-earth complexes, and the same explanations are given.

As for the mesophase of $\mathbf{L}_{III}$, in the X-ray diffraction pattern recorded at 80 °C, two sharp, small-angle reflections of high intensity, in the ratio 1:2, attributed to the lamellar periodicity ($d = d_{001} = 50.0$ Å) and to its first harmonics ($d_{002} = 25.0$ Å) were observed (Figure 4). This periodicity of 50 Å corresponds to a multilayered smectic phase formed by the piling of phenanthroline- and cyanobiphenyl-containing sublayers alternating with the aliphatic spacer sublayer. Additionally, broad reflections at ca. 14 Å (d in Figure 4) and at 4.6 Å were observed. The reflection at 4.6 Å corresponds to the usual lateral periodicity within the molten chains sublayer, whereas the reflection at 14 Å corresponds to some lateral periodicity within the sublayer occupied by the phenanthroline groups, very likely to a ribbon's width of stacked phenanthrolines. This latter assumption is supported by the fact that phenanthroline-like cores show, like other discotic cores, a strong tendency to stack into columns to give columnar phases with typical stacking periodicities ranging between 3.3 and 3.6 Å.[31] Indeed, the peak located at 4.6 Å is much wider than in classical disordered smectic phases as the wing of the signal extends to ca. $2\theta = 30°$. The peak shape analysis eventually reveals a superposition of two broad signals, that of 4.6 Å and another weak one at 3.3−3.5 Å (see the figure in the Supporting Information).

To have a more precise description of the molecular arrangement, a quantitative discussion based on the measured periodicities and calculated partial molecular volumes is proposed. Given the alternate packing of the phenanthroline rings, it is therefore necessary to consider two molecules in a head-to-tail arrangement to calculate the area occupied by the three terminal mesogenic units at the interface between the smectic layers. Such an area $A = 2V_M/d$ is directly deduced from the molecular volume ($V_M \approx 2400$ Å^3 estimated at 80 °C) and the layer thickness ($d = 50$ Å) and is found to be ca. 96 Å^2. This calculation thus gives a molecular area per mesogenic unit of 32 Å^2, which is larger than the well-known cross section of the cyanobiphenyl groups of about 20−24 Å^2. In this case, the sublayers containing the cyanobiphenyl groups are either partially interdigitated, as in the case of the SmA_d phase,[32] or the aliphatic spacers and the cyanobiphenyl groups are tilted with an angle of about ($\psi \approx 50°$) but without any correlation in the tilt direction, as in the SmA phase of the de Vries type. Let us recall that in the de Vries SmA phase, the molecules are assumed to be tilted as in the SmC phase resulting from either tilted layers being stacked in a random fashion[33] or the molecules being tilted without long-range order in the direction of tilt within the layer.[33,34]

In the case of the phenanthroline-rich slabs, the macrocycles occupy a transverse area of 48 Å^2 and are packed in such a way that short columns are formed. The ratio of this transverse area with the ribbon periodicity in the X-ray diffraction pattern (14 Å) gives a stacking periodicity of 3.4 Å (within the ribbons). The particular nature of this arrangement in layers was found consistent with molecular dynamics calculations, for which a density of 1 was found. A snapshot of this modelized structure is shown in Figure 5.

This smectic phase cannot be simply referred to as a classical SmA phase due to the presence of the short columns within layers. Such unusual structure is similar to the SmA phase formed by the charge transfer assembly of tetrathiofulvalene and tetracyanoquinodimethane reported by Davidson et al.[35] and that formed by ortho-palladated bipyridine[36] and dicopper bis-(terpyridine)[2c] complexes reported by Ziessel and co-workers in which the aromatic cores of the molecules stacked into small columns randomly oriented within smectic layers. Therefore, the mesophase would be more appropriately defined as a *lamellar phase with* short-range columnar order within the layers, i.e., a *lamello-columnar phase*[37] and labeled SmA_{Col} phase.

The rhenium(I) complexes also exhibit an interesting thermal behavior, which is extremely dependent on the ligand type. The first derivative, based on $\mathbf{L}_I$, $[Re(CO)_3Br\mathbf{L}_I]$, exhibits a high-temperature monotropic nematic phase as recognized by POM. The nematic phase was thus strongly destabilized upon complexation to rhenium pentacarbonyl bromide. The rhenium(I) complex of $\mathbf{L}_{II}$, $[Re(CO)_3Br\mathbf{L}_{II}]$, exhibits an enantiotropic nematic phase and a monotropic smectic-like phase. Not unambiguously ascertained by POM alone, both mesophases were eventually fully identified by the combination of both POM and XRD techniques. The X-ray diffraction patterns of the nematic phase recorded at

(31) Weber, P.; Guillon, D.; Skoulios, A. *Liq. Cryst.* **1991**, *9*, 369.
(32) (a) Seurin, P.; Guillon, D.; Skoulios, A. *Mol. Cryst. Liq. Cryst.* **1981**, *71*, 37. (b) Guillon, D.; Skoulios, A. *Mol. Cryst. Liq. Cryst.* **1983**, *91*, 341. (c) Hardouin, F.; Levelut, A. M.; Achard, M. F.; Sigaud, G. *J. Chim. Phys.* **1983**, *80*, 53. (d) Hardouin, F. *Physica A* **1986**, *140*, 359.
(33) De Vries, A. *Mol. Cryst. Liq. Cryst.* **1977**, *41*, 27.
(34) De Vries, A. *Mol. J. Chem. Phys.* **1979**, *71*, 25.
(35) Davidson, P.; Levelut, A. M.; Strzelecka, H.; Gionis, V. *J. Phys. (Orsay, Fr.)* **1983**, *44*, 823.
(36) El-ghayoury, A.; Douce, L.; Skoulios, A.; Ziessel, R. *Angew. Chem., Int. Ed.* **1998**, *37*, 1255.
(37) Tschierske, C. *Annu. Rep. Prog. Chem., Ser. C* **2001**, *97*, 191.

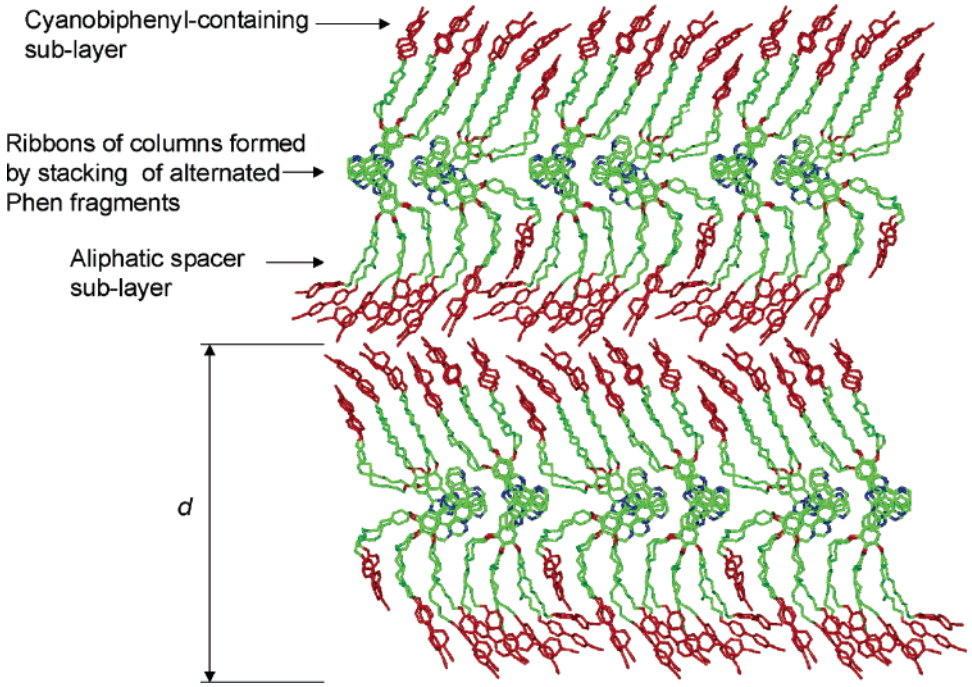

Figure 5. Representation of the alternated packing of $\mathbf{L}_{III}$ in the SmA_{Col} phase built from two snapshots of a single layer obtained by MD calculations. The columns forming ribbons can be seen from the alternated stacking of the phenanthroline macrocycles. The cyanobiphenyl mesogens are randomly tilted (see text).

80, 100, and 120 °C are similar to the patterns obtained with the other nematogens, but in addition local orderings consisting of *cybotactic* smectic clusters were observed. This local layering was in fact heralding the formation of a lower-temperature smectic-like phase. Indeed, the pattern recorded at 60 °C on cooling, revealed two sharp, weakly intense, small-angle reflections, in the ratio 1:2, which are characteristic of a layered structure, with a periodicity d of 45.3 Å. In addition, weak and diffuse signals in the wide-angle part were detected at about 4.6 and 3.3 Å corresponding to the lateral short-range order of the molten chains and cyanobiphenyl groups and to the alternated stacking of the phenanthroline rings, respectively, as for $\mathbf{L}_{III}$. The supramolecular organization of the complex within the smectic phase thus resembles that of the ligand $\mathbf{L}_{III}$ described above (SmA_{Col} phase), with an alternation of mesogenic-rich layers and phenanthroline−metal layers. The same analysis as above, by estimating the molecular volume close to 1900 $Å^3$, gives a molecular area, $A = 2V_M/d \approx 84$ $Å^2$. This results in a molecular area per mesogenic unit of 42 $Å^2$, which is large (about twice) compared to the transverse cross section of one cyanobiphenyl group (20−24 $Å^2$). This therefore suggests that the packing of the mesogens within the sublayer can be most likely described as a nontilted monolayer (i.e., a layer containing one thickness of cyanobiphenyls) with complete interdigitation of the cyanobiphenyl groups from the molecules of adjacent layers (ziplike), and it is now consistent with an area per mesogenic groups of 21 $Å^2$. In the case of the phenanthroline/rhenium-rich slabs, the macrocycles transverse area is also 42 $Å^2$, which is smaller than in the $\mathbf{L}_{III}$ ligand case, despite the bulky metallic fragment. This could indicate an out-of-plane tilting of the piled macrocycles. A representation of this molecular arrangement in the SmA_{Col} phase is shown, for which the likeliness is supported by MD calculations (Figure 6).

Finally, the $[Re(CO)_3Br\mathbf{L}_{III}]$ complex exhibits a mesophase, but the strongly birefringent and sandlike texture seen by POM was not characteristic of any particular mesophase. The use of hydrophilic and hydrophobic treated glass slides did not help for a concluding assignment either. The X-ray diffraction pattern recorded at 80 °C (Figure 7), shown as a representative example of the different temperatures at which the experiment was done, contains a set of five sharp reflections and four scattering halos (Table 2). The sharp reflections (1−5) in the low-angle region were indexed in the following 2D rectangular lattice with the parameters $a = 82.0$ Å, $b = 36.7$ Å, $S = 3010$ $Å^2$ (Figure 8). The broad signal 7 in the wide-angle part detected at about 4.5 Å corresponds to the lateral short-range order of the molten chains and cyanobiphenyl groups (D_0). The reflection 8 ($h_0 = 3.3$ Å) corresponds to the stacking of the phenanthroline macrocycles into columns. From the FWHM of this reflection, a correlation length of about 100 Å is deduced, corresponding to columns of about 30 phenantroline units. Moreover, the spacing of reflection 8 corresponds to the distance between macrocycles, being very close to the value found for analogous phenantroline-containing compounds in the crystalline state or for other macrocycles in columnar phases in general.[31] This indicates that the scattering vector is nearly parallel to both the columnar axis and the normal to the macrocycle's plane and that, consequently, these species are quasi not tilted within the columns. The piling of the sublayers containing the columns formed by the phenanthroline complexes and of the cyanobiphenyl-containing sublayers alternating with aliphatic sublayers (spacer) has an overall periodicity of $a/2$ (i.e., d_{20}). This attribution is justified by the absence of the (10) and (30) reflections and by the surprisingly high intensity of the (40) reflection with respect to the (20) reflection, consistent with a peak of electronic density associated to the cyanobiphenyl

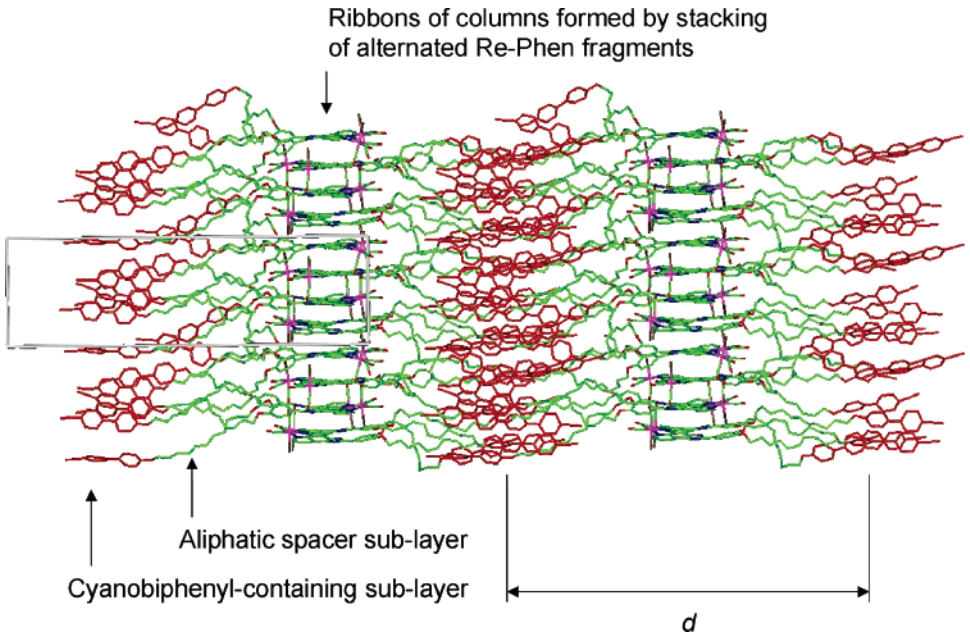

Figure 6. Snapshot of the packing of [Re(CO)$_3$Br**L**$_{II}$] in the alternated SmA$_{Col}$ phase obtained from MD calculations. Short columns forming ribbons can be seen from the alternated stacking of the phenanthroline macrocycles.

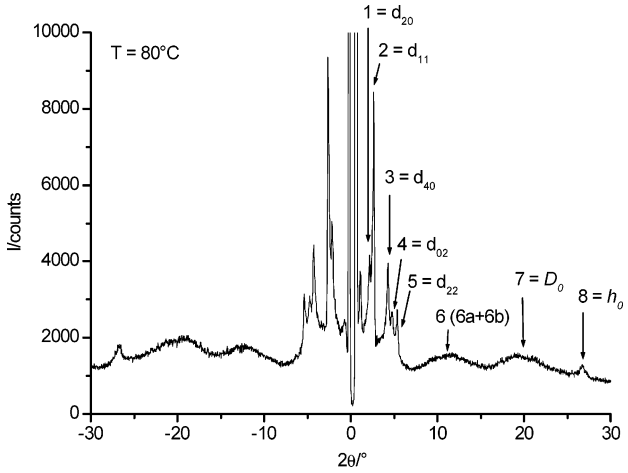

Figure 7. Representative X-ray diffraction pattern of the Col$_r$L phase of [Re(CO)$_3$Br**L**$_{III}$] at 80 °C.

Table 2. Low- and Wide-Angle Bragg Reflections Collected from the X-ray Diffraction Pattern of [Re(CO)$_3$BrL**$_{III}$] at 80 °C**

reflection[a]	d_{meas}/Å[b]	I[c]	L[c]	hk[c]	d_{calc}/Å[b]	assignment
1	41.0	M	S	20	41.0	rectangular lattice
2	33.5	VS	S	11	33.5	rectangular lattice
3	20.55	M	S	40	20.5	rectangular lattice
4	18.6	W	S	02	18.35	rectangular lattice
5	16.6	W	S	22	16.75	rectangular lattice
6a	8.8					$\sim 2D_0$
6b	6.7					$\sim 2h_0$
7	4.5		22			D_0
8	3.3		100			h_0

[a] Reflection number. [b] d_{meas} and d_{calc} are the measured and calculated diffraction spacing. [c] I is the intensity of the reflections: VS, very strong; M, medium; W, weak; L, sharp reflection (S) or correlation length value obtained from the Scherrer Guinier-modified formula; hk are the indexations of the reflections. D_0, average mesogen distance; h_0, average stacking distance.

sublayers. Finally, another broad signal (6) is observed between 7° and 15° (2θ) whose shape allows the decomposition into two diffuse reflections centered around ca. 8.8−9.0 Å (6a) and ca. 6.7−7.0 Å (6b), respectively (vide infra).

In contrast to classical discotic molecules, the amphipatic moiety is connected to only one side of the phenantroline ring. This results in the microsegregation of the rhenium−phenantroline complexes and of the amphipatic moieties in adjacent sublayers. Again, the packing corresponds to a lamellar columnar phase consisting in the superposition of two types of sublayers separated by the aliphatic continuum stemmed by the spacer: one slab contains the columns formed by the complexes, and the other one accommodates the cyanobiphenyl mesogens. This packing is thus similar to that described above for **L**$_{III}$ and [Re(CO)$_3$Br**L**$_{II}$], except that the short-range correlated ribbons of stacked phenantroline macrocycles are replaced by the long-range correlated two-dimensional rectangular organization of the columns formed by the stacked rhenium−phenantroline complexes. Therefore, and for consistency with the previous results, we may label this *lamellar columnar phase* as Col$_r$L since both the columnar and lamellar orderings are long-range correlated.

In the crystalline phase of related compounds such as the chlorotricarbonyl(1,10-phenantroline)rhenium(I), 6.5 Å is the minimum rhenium−rhenium distance.[38] This value is also twice the distance corresponding to the stacking of the macrocycles (6b, $2h_0 = 6.6$ Å). Therefore, neighboring macrocycles within the columns have to stack with a shift on their orientation around the columnar axis. As in phthalocyanine systems packed in columnar phases,[31] a signal corresponding to this additional dimer's periodicity is expected in the diffractogram; and indeed, this distance corresponds to the location of the reflection 6b (vide supra). For the description of the packing within the sublayers, the molecular area and the number of molecules per slice of section $a \times b$ and of thickness 2×3.33 Å (from the alternated stacked phenanthrolines) need to be calculated. The volume of this slice (ca. 20 000 Å^3) corresponds to an

(38) Haddad, S. F.; Marshall, J. A.; Crosby, G. A.; Twamley, B. *Acta Crystallogr., Sect. E* [Online] **2002**, *58*, 559−CCDC 198307.

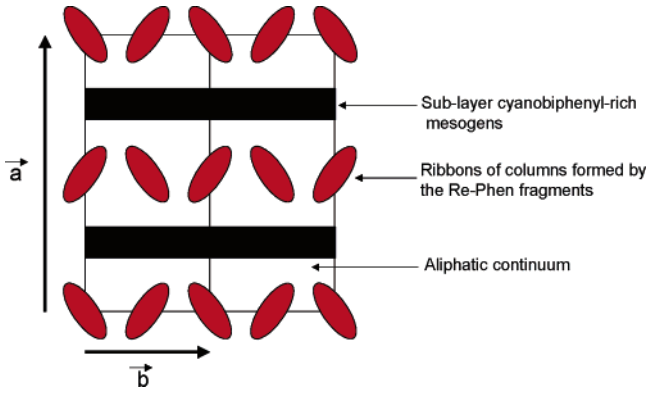

Figure 8. Model representing the Col_rL phase of [$Re(CO)_3Br\mathbf{L}_{III}$]: in red, elliptic cross sections of the columns formed by the stacking of the rhenium−phenanthroline fragments, arranged in a rectangular lattice ($\vec{a}$, $\vec{b}$) with the *p2mg* plane group; in black, sublayers formed by the cyanobiphenyl mesogenic units. The rest of the lattice is occupied by the aliphatic chains.

occupation of eight molecules of 2500 Å^3 in consistency with the molecular volume determination. Since the lattice contains two sublayers of cyanobiphenyl mesogens and each molecule three of these mesogens, about twelve mesogens are contained in a sublayer slice 6.7 Å thick. This corresponds to a molecular area of $36.7 \times 2 \times 3.33/12 = 20.4$ Å^2, which is consistent with the transverse cross section of one cyanobiphenyl group (20−24 Å^2). This value of the molecular area per mesogen is identical to that found for the rhenium complex [$Re(CO)_3Br\mathbf{L}_{II}$] discussed previously, and therefore the packing of the mesogens within the sublayer can also be classed as a nontilted monolayer case. Again, this up and down arrangement of the mesogens within such a totally interdigitated monolayer results in a doubling of the in-plane periodicity, and the corresponding signal is expected in the X-ray pattern; indeed, this distance corresponds to the position of reflection 6a ($6a = 2D_0 = 8.8$ Å).

From this complete analysis, the rectangular lattice contains four columns of stacked rhenium−phenantroline complexes and the average intercolumnar distance is therefore equal to $b/2$, i.e., 18.3 Å. This value is larger than the 14 Å found for the average ribbon periodicity in the ligand's pattern: in this case, the discrepancy corresponds to the organization of the rhenium−bromotricarbonyl moiety between the columns. The doubling of the lattice along both the *a* axis and *b* axis is revealed by the presence of the reflection (11), while the reflections (10) and (01) are absent. This lattice doubling should result from different repartitions of the electronic density around the columns. Moreover, it would probably be related to the organization on the electron-rich rhenium moiety, since the reflection (11) is highly intense. As the most simple columnar organization consistent with the lattice doubling, the following schematic view of a packing with a *p2mg* symmetry is proposed (Figure 8). The ellipsoid center coincides with the columnar axis, and the ellipsoid ends stand for a peak of electronic density.

Luminescence Properties. The trivalent lanthanide ions are well-known for their intense luminescence. This luminescence is not only of interest for optical applications, but the fine structure in the luminescence spectrum of the europium(III) can also be used to probe the symmetry of the first coordination sphere of rare-earth complexes. The

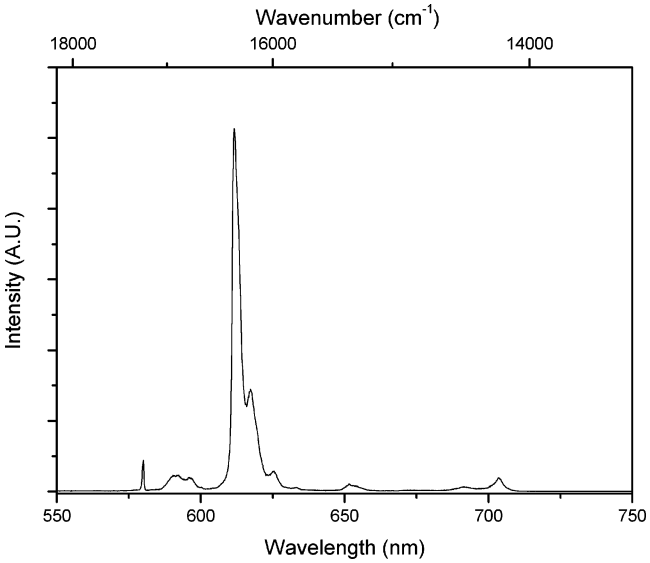

Figure 9. Luminescence spectrum of [$Eu(tta)_3\mathbf{L}_I$] in the solid state at room temperature. The excitation wavelength is 350 nm.

luminescence spectrum of europium(III) is sensitive to small structural changes in the first coordination sphere. The luminescence properties of the mesomorphic neodymium(III), samarium(III), europium(III), erbium(III), and ytterbium(III) compounds were studied in the solid state at room temperature. The spectroscopic and photophysical properties of these complexes are very comparable with those of the [$Ln(tta)_3(phen)$] complexes, where Ln = Nd, Sm, Eu, Er, Yb, tta = 2-thenoyltrifluoroacetonate, and phen = 1,10 phenanthroline. Although both the samarium(III) and europium(III) compounds emit in the visible spectral region, the red europium(III) luminescence is much brighter than the reddish samarium(III) luminescence. These findings are in agreement with the fact that [$Eu(tta)_3(phen)$] is one of the best-performing red-emitting molecular luminescent materials. Because most of the luminescence output is concentrated in the $^5D_0 \rightarrow {}^7F_2$ transition of Eu^{3+}, the red color is very bright and has a high monochromaticity. The luminescence quantum yield of the complexes dissolved in DMF was calculated and compared with that of the [$Eu(tta)_3(phen)$] complex. The values are 28 (± 2)%, 19 (± 2)%, and 23 (± 1)% for the europium(III) complexes of the ligands $\mathbf{L}_I$, $\mathbf{L}_{II}$, $\mathbf{L}_{III}$, respectively. The luminescence quantum yield reported for [$Eu(tta)_3(phen)$] in DMF is 36%.[39] The addition of the imidazole ring makes the energy transfer less favorable, but the systems remain efficient luminescent materials with a good luminescence quantum yield.

The luminescence spectrum of the compound [$Eu(tta)_3\mathbf{L}_I$] is shown in Figure 9. The fact that only one emission peak is observed for the $^5D_0 \rightarrow {}^7F_0$ transition (580 nm) in the three europium(III) complexes we studied is a good indication that the local surroundings of all the europium(III) ions are very similar. Only two crystal-field transitions are observed for the $^5D_0 \rightarrow {}^7F_2$ transition (612 nm), but the broadening of the crystal-field transition at the high-energy side (shorter wavelengths) indicates that there are two overlapping crystal-

(39) Filipescu, N.; Mushrush, G. W.; Hurt, C. R.; McAvory, N. *Nature* **1966**, *211*, 960.

field transitions. The degeneracy of the $^7F_1$ level (observable in the $^5D_0 \rightarrow {}^7F_1$ transition at 592 nm) is totally removed so that the Eu^{3+} is a site of low symmetry (orthorhombic or lower). The intensity ratio $I(^5D_0 \rightarrow {}^7F_2)/I(^5D_0 \rightarrow {}^7F_1)$ is 15.4, 10.8, and 14.8 for the complexes $[Eu(tta)_3\mathbf{L}_I]$, $[Eu(tta)_3\mathbf{L}_{II}]$, and $[Eu(tta)_3\mathbf{L}_{III}]$ respectively. Changes induced by the extra side chains appear to have an influence, but the values are also comparable to the values calculated for $[Eu(tta)_3(phen)]$ and $[Eu(tta)_3(H_2O)_2]$. These complexes have a ratio of 11 and 18, respectively. The luminescence lifetime of the $^5D_0 \rightarrow {}^7F_2$ transition was determined by measurement of the luminescence decay curves. Values of 278 ($\pm$ 8) μs, 327 ($\pm$ 10) μs, and 282 ($\pm$ 9) μs was found for the monoexponential decay curves of the europium complexes $[Eu(tta)_3\mathbf{L}_I]$, $[Eu(tta)_3\mathbf{L}_{II}]$, and $[Eu(tta)_3\mathbf{L}_{III}]$ respectively. These decay times are very similar. It can be concluded that the mesogenic groups have a small influence on the spectroscopic properties, but overall there is no indication that there are systematic changes. Small, local variations in the first coordination sphere are responsible for the different luminescence behavior.

The neodymium(III), erbium(III), ytterbium(III), but also the samarium(III) are emitting in the near-infrared. These ions show luminescence in the telecommunication low-loss regions of silica. Luminescence can be observed for the complexes of these trivalent lanthanide ions with ligands $\mathbf{L}_I$, $\mathbf{L}_{II}$, and $\mathbf{L}_{III}$. The luminescence of the erbium(III) complexes is the most difficult to measure, but the energy transfer in the mesogenic systems is efficient, and luminescence can be observed at 1530 nm. Spectra and lifetime measurements are available in the Supporting Information.

The lanthanide(III) complexes of the ligands $\mathbf{L}_I$, $\mathbf{L}_{II}$, and $\mathbf{L}_{III}$ are well soluble in the nematic liquid host 4′-pentyl-4-cyanobiphenyl (5CB). Although we did not determine quantitative solubility values, the solubility of the complexes described in this paper is much higher than the solubility of the parent $[Ln(tta)_3(phen)]$ complexes.[40] This good solubility in comparison with that of other lanthanide(III) complexes can be explained by the structural similarities between the host matrix and the guest molecules. After all, each lanthanide complex contains 4-cyanobiphenyl groups attached to the periphery of the 1,10-phenanthroline group and exhibits a nematic phase. Luminescent liquid-crystal mixtures can be obtained by doping the lanthanide complexes into the liquid-crystal host matrix. Heating the sample above the clearing point of the liquid-crystal host 5CB led in this case to a decrease in luminescence intensity. This decrease is larger than what can be expected from the decrease of the luminescence intensity by a stronger radiationless deactivation of the excited states of the lanthanide(III) ion. The decrease in luminescence intensity is due to the less pronounced scattering of the excitation light in the isotropic liquid than in the mesophase. When there is more scattering of the excitation light, more light can be absorbed by the ligand chromophores of the lanthanide complexes. So far, only limited literature data on the spectroscopic and photophysical properties of adducts of tris β-diketonato lanthanide(III) complexes with 2-arylimidazo[f]1,10-phenanthrolines are available in comparison with the adducts of 1,10-phenanthroline.[41] The main differences of the 2-arylimidazo[f]1,10-phenanthroline adducts with respect to the 1,10-phenanthroline adducts is the more extended conjugation in the former molecules, which results in different positions of the ligand triplet levels and an altered energy transfer to the lanthanide ions.

Conclusions

In this paper, several liquid-crystalline metal complexes with a high coordination number (eight or nine) have been obtained by attaching mesogenic groups via a flexible alkyl spacer to the coordinating unit. The approach is illustrated for rhenium(I) complexes and for rare-earth complexes. Although we have chosen the 4-cyanobiphenyl group as the mesogenic promotor and a 1,10-phenanthroline derivative as the coordinating group, the concept of decoupling of the mesophase-inducing groups and the coordination groups can be extended to other mesogenic groups and ligands. Examples of possible mesogenic groups can be 4-alkoxybiphenyl or cholesteryl derivatives. This concept is different from other studies on metallomesogens, where the key idea to obtain high coordination number metallomesogens is to increase the number of long alkyl chains attached to the central metal core. The advantage of our approach is that in our case metallomesogens showing a nematic phase can be obtained, whereas metallomesogens with a large number of long alkyl chains often form columnar mesophases. Unconventional phases were also obtained for the rhenium complexes bearing two or three cyanobiphenyl side-groups. An interesting feature of the rare-earth complexes studied in this work is their good solubility in nematic liquid-crystal solvents so that by a doping procedure luminescent liquid crystals can be obtained. In these anisotropic solvents, the crystal-field fine structure of the dissolved lanthanide complexes is well resolved.

Acknowledgment. K.B., T.N.P.V., and K.D. thank the FWO-Flanders (Belgium) for a postdoctoral fellowship. T.C. is research assistant of the FWO-Flanders. Financial support by the F.W.O.-Flanders (G.0117.03) and by the K.U. Leuven (GOA 03/03) is gratefully acknowledged. B.H., C.B., D.G., and B.D. thank the CNRS and ULP for support and funding. Funding for travel was obtained via a Tournesol project (Project T2004.10). Mass spectra were measured by Ms. Leen Van Nerum. CHN analyses were performed by Mrs. Petra Bloemen.

Supporting Information Available: Experimental section with general experimental details, the description of the synthetic procedures, NMR spectra, defect textures of mesophases as observed by polarizing optical microscopy, luminescence spectra, XRD diffractograms and additional structural models. This material is available free of charge via the Internet at http://pubs.acs.org.

CM0513177

(40) (a) Binnemans, K.; Moors, D. *J. Mater. Chem.* **2002**, *12*, 3374. (b) Van Deun, R.; Moors, D.; De Fré, B.; Binnemans, K. *J. Mater. Chem.* **2003**, *13*, 1520.

(41) (a) Gao, D. Q.; Bian, Z. Q.; Wang, K. Z.; Jin, L. P.; Huang, C. H. *J. Alloys Compd.* **2003**, *358*, 188. (b) Bian, Z. Q.; Wang, K. Z.; Jin, L. P. *Polyhedron* **2002**, *21*, 313.